

Controllable spin-current blockade in a Hubbard chain

Yao Yao,¹ Hui Zhao,^{1,2} Joel E. Moore,^{3,4} and Chang-Qin Wu^{1,*}

¹*Department of Physics and Surface Physics Laboratory, Fudan University, Shanghai 200433, China*

²*Department of Physics, Tongji University, Shanghai 200092, China*

³*Department of Physics, University of California, Berkeley, California 94720, USA*

⁴*Materials Sciences Division, Lawrence Berkeley National Laboratory, Berkeley, California 94720, USA*

(Received 2 October 2008; published 26 November 2008)

We investigate the spin or charge transport in a one-dimensional strongly correlated system by using the adaptive time-dependent density-matrix renormalization-group method. The model we consider is a non-half-filled Hubbard chain with a bond of controllable spin-dependent electron hoppings, which is found to cause a blockade of spin current with little influence on charge current. We have considered (1) the spread of a wave packet of both spin and charge and (2) the spin and charge currents induced by a spin-dependent voltage bias. It is found that the spin-charge separation plays a crucial role in the spin-current blockade, which may be utilized to observe the spin-charge separation directly.

DOI: [10.1103/PhysRevB.78.193105](https://doi.org/10.1103/PhysRevB.78.193105)

PACS number(s): 73.23.Hk, 71.10.Fd, 71.10.Pm, 72.25.-b

In one-dimensional (1D) strongly correlated systems, an essential phenomenon is the spin-charge separation (SCS),¹ which is believed to play a central role in 1D transport.² To study transport problems in 1D systems, the characteristics of SCS must be taken into account. However, due to the limitations of existing methods, the discussion in the past has been limited to a few simple cases; an example is the significant work by Kane and Fisher³ on scaling properties of tunneling through a spin-symmetric point impurity in a fermion system. Hence more powerful methods are needed to compute transport properties beyond scaling and to treat a general interacting Hamiltonian. Furthermore, spin-dependent transport problems have attracted increasing interest in the last two decades; many proposed spintronics devices^{4,5} require the manipulation of spin currents, which are naturally decoupled from charge currents in 1D systems. On the other hand, a number of experimental works have sought to observe the phenomenon.⁶ Rapid progress in ultracold atomic gas experiments^{7,8} makes it possible to see SCS in a new context.⁹

Recently, the adaptive time-dependent density-matrix renormalization group (t-DMRG) (Refs. 10 and 11) was developed by combining the DMRG method¹² with quantum information concepts. The key idea of this method is to break up the evolution operator with Trotter decomposition,¹³ then apply it to the states within a DMRG configuration. With the method as well as other real-time evolution ones within DMRG, there have been a number of investigations on transport properties in 1D strongly correlated or impurity systems, including spin-1/2 chains,¹⁴ Bose-Hubbard model,¹⁵ and quantum switch.¹⁶ The dynamical problems with impurities were also studied widely using static DMRG method embedding with persistent current^{17,18} and functional renormalization group.^{18,19} An interesting result that partly motivates our study was the study of SCS by Kollath *et al.*²⁰ In conventional treatment with the bosonization method, only low-energy excitations were considered. The above study goes beyond the low-energy excitation spectrum by considering the evolution of a “big” (multiparticle) wave packet that shows the SCS phenomenon.²⁰

In this Brief Report, we propose to consider a non-half-

filled Hubbard chain in which one special bond has controllable spin-dependent electronic hoppings, motivated both by the development of optical lattices of ultracold atoms in which all hoppings can be controlled and the need to control spin currents for the application in spintronics. By using the adaptive t-DMRG method, we simulate the spread of a wave packet as well as the spin and charge currents under a spin-dependent voltage bias. The most significant result we find is that the spin-current blockade can be realized by adjusting the spin-dependent hopping on that special bond while the charge current has not been affected.

The system we are considering is described by the following Hamiltonian:

$$H_S = - \sum_{i,\sigma} t_{i,i+1}^\sigma (c_{i,\sigma}^\dagger c_{i+1,\sigma} + \text{h.c.}) + U \sum_i n_{i,\uparrow} n_{i,\downarrow}, \quad (1)$$

where $c_{i,\sigma}^\dagger (c_{i,\sigma})$ creates (annihilates) an electron with spin $\sigma (= \uparrow, \downarrow)$ on the i th site, $n_{i,\sigma} (= c_{i,\sigma}^\dagger c_{i,\sigma})$ is the corresponding electron number operator, the hopping constants $t_{i,i+1}^\sigma \equiv t_0$ on all bonds but a special bond ($i = l_s$), where $t_{i,i+1}^\sigma (= t_\sigma)$ is an adjustable spin-dependent quantity, which introduces a local magnetic moment, like a spin-dependent Anderson impurity. Without the special bond, the Hamiltonian is nothing but the usual 1D Hubbard model with $U (> 0)$ being the on-site repulsive Coulomb interaction. Without loss of generality, we keep $t_\uparrow = t_0$ while t_\downarrow is adjusted from t_0 to 0. Although there has been some similar scheme on the spin-dependent impurity,¹⁶ we present a possible proposal in Fig. 1 on the realization of this model in an optical lattice. In the lattice, the spin-up and spin-down atoms could be trapped in a pair of parallel period potential wells created by interfering linear-polarized laser beams.⁸ Hence, one might change the laser beam to rotate half of spin-down atoms around the spin-up atom axis by an angle θ , which reduces the spin-down atom hopping at the special bond. It is clear that t_\downarrow of this special bond in Eq. (1) could be easily adjusted by changing θ .²¹

In the following, we will apply the t-DMRG method with second-order Trotter decomposition to simulate the dynamical

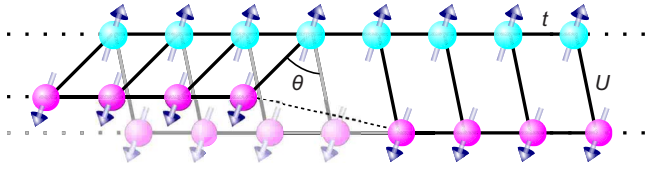


FIG. 1. (Color online) The realization of a Hubbard chain with a special bond of controllable spin-dependent electronic hopping in an optical lattice. The rotation of the left spin-down atoms around the spin-up atom axis reduces the spin-down atom hopping at the special bond, i.e., the t_{\perp} in Eq. (1) decreases as the angle θ increases.

cal evolution. The number of sites (L) is always taken to be 176 while the number of electrons (N_e) is 116; the corresponding filling factor [$N_e/(2L)$] is about 1/3, so the system is at Luttinger liquid phase. The time step is taken as 0.04 (in unit of \hbar/t_0) and the number of kept DMRG states (M) is chosen to be large enough to ensure the error being less than $O(10^{-3})$. The spin and charge currents, the quantities we focus on in this calculation, are defined as $J_{c,s}(j) = J_{\uparrow}(j) \pm J_{\downarrow}(j)$, where

$$J_{\sigma}(j) \equiv it_{j,j+1}^{\sigma} \langle c_{j,\sigma}^{\dagger} c_{j+1,\sigma} - c_{j+1,\sigma}^{\dagger} c_{j,\sigma} \rangle. \quad (2)$$

First, we consider the spread of a wave packet as done by Kollath *et al.*,²⁰ but in a Hubbard chain with a bond of controllable spin-dependent electron hoppings, described by Eq. (1). The wave packet is induced by the spin-dependent Gaussian potential

$$H_P = -P \sum_i \exp\left[\frac{-(i-l_p)^2}{2l_d^2}\right] \hat{n}_{i,\uparrow}, \quad (3)$$

which acts only on the spin-up electrons, so that it carries both of spin and charge. Then the potential will be switched off and the wave packet will be spread according to the time-dependent many-body Schrödinger equation. Clearly P determines the potential strength, l_p the center of the induced wave packet, and l_d its width.

In Fig. 2, we show the spin and charge currents at various times for $t_{\perp}=0$. The initial potential locally on the spin up generates simultaneously spin and charge wave packets and then the wave packets will split into two parts and propagate to opposite directions, respectively.²⁰ Since the potential strength P we took is not large, the spin and charge density of this wave packet is very small, but the currents defined in Eq. (2) show the propagation of this wave packet very clear. In Fig. 2(a), we show the current distribution at a time before the spin and charge reach the special bond. The split of the two peaks indicates the different speeds of spin and charge excitations, so that the spin-charge separation is observed clearly. Next we will see clearly from the figure the charge current goes through the special bond almost freely, while the spin current is blocked by the special bond. A spin current reflecting at the special bond is shown in the figure by its value being changed from positive to negative. The change in charge currents from negative to positive indicates the charge reflection at the left end since we use an open boundary condition for the chain.

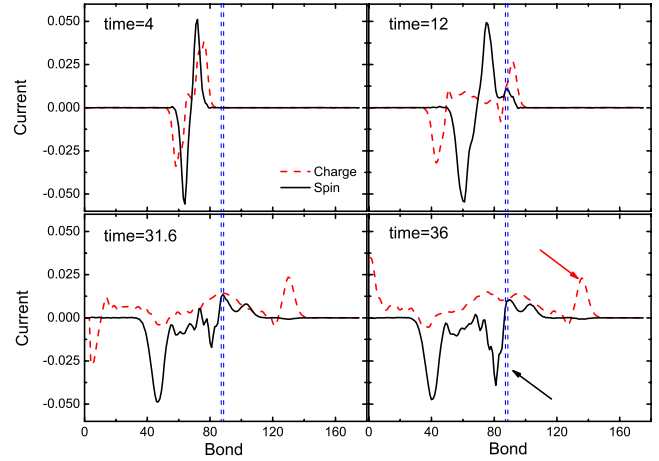


FIG. 2. (Color online) The spin (solid line) and charge (dashed line) current in the spread of a wave packet with $P=0.8t_0$, $l_d=1$, $l_p=62$ for $U=8t_0$. The location of this special bond is indicated by a double dashed (blue) line. Positive (negative) values imply the current flows to the right (left). The dashed (red) arrow indicates the charge transmitted through while the solid (black) one the spin reflected from the special bond.

We argue that, in the following, the spin-current blockade we observe here only happens in a strongly correlated system. It is different from the “spin blockade” effect,²² which is merely spin-related Coulomb blockade. To understand the phenomenon we observed above, we consider the large U limit of the Hubbard-type model in Eq. (1), which leads to the so-called t - J model $H_{t,J} = H_t + H_J$, where H_t is the hopping term in Eq. (1) and

$$H_J = -\frac{1}{U} \sum_{ijkss'} t_{ij}^s t_{jk}^{s'} c_{is}^{\dagger} c_{js} n_{j\uparrow} n_{j\downarrow} c_{js'}^{\dagger} c_{ks'} \quad (4)$$

with $t_{ij}^s \equiv t_{i,i+1}^s \delta_{i,j-1} + t_{i-1,i}^s \delta_{i,j+1}$.²³ This model works on the space that has projected out all configurations with at least one doubly occupied site for a less-than-half filling system and is responsible for the low-energy excitations of the model in Eq. (1). It is well known that the hopping term H_t is responsible for the charge excitations while H_J controls the spin excitations, and that for the usual Hubbard model, H_J corresponds to a Heisenberg spin chain. Writing

$$\vec{S}_i \cdot \vec{S}_j \equiv S_i^z S_j^z + \frac{1}{2}(S_i^+ S_j^- + S_i^- S_j^+), \quad (5)$$

the second term is responsible for the spin-exchange process that is necessary for an S_z spin current. Based on H_J in Eq. (4) from the large- U expansion, we show the spin-exchange process in Fig. 3, in which there is a virtual intermediate state, so electronic hoppings for both spins are necessary for the process via a virtual state. Then it is clear that spin current is blocked at the special bond when $t_{\perp}=0$ since only spin-up electrons can hop across the special bond.

Now, we come to the calculation of spin and charge currents under a spin-dependent voltage bias, for which we con-

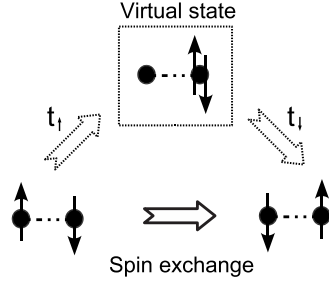


FIG. 3. A spin-exchange process that is necessary for the spin current in the strong-interaction limit.

sider the system of a Hubbard chain with a special bond attached with two ideal leads at its two end, which is described by the following Hamiltonian:

$$H = H_S + H_{\text{lead}} + H_{\text{int}}, \quad (6)$$

where H_S has been given in Eq. (1) and the summation over site index runs from 1 to L_S with L_S being the size of the Hubbard chain, $H_{\text{lead}} \equiv H_L + H_R$ and

$$H_\alpha = -t_0 \sum_{i,\sigma \in \alpha} (c_{i,\sigma}^\dagger c_{i\pm 1,\sigma} + \text{h.c.}) - \sum_{i,\sigma \in \alpha} V_\sigma^\alpha n_{i,\sigma}, \quad (7)$$

with $\alpha=L$ or R and the sign \pm taking $-(+)$ for $\alpha=L(R)$, and

$$H_{\text{int}} = -t_0 \sum_{\sigma} (c_{0,\sigma}^\dagger c_{1,\sigma} + c_{L,\sigma}^\dagger c_{L+1,\sigma} + \text{h.c.}). \quad (8)$$

The spin-dependent voltage bias $V_\sigma \equiv V_\sigma^L - V_\sigma^R$ applied at the two leads turns on at $t=0$, so that currents appear gradually at the same time and reach constant values finally. In the calculation, we take $V_\downarrow=0$ and $V_\uparrow=0.1t_0$, without loss of generality, to induce both spin and charge currents through the Hubbard chain. This nonzero voltage bias fixes an energy scale in the field-theoretical treatment of tunneling in a Luttinger liquid,³ which cuts off the renormalization-group flow of the tunneling probability. The dominant effect found in the time evolution from this initial condition is the spin blockade discussed above, but it may be possible by varying voltage bias to observe the predicted power-law dependence of transmission on voltage bias (or temperature).³

Now we show in Fig. 4 the spin and charge currents at various times for different Hubbard chain lengths (L_S) or the numbers of kept DMRG states (M) in the calculations induced by the spin-dependent voltage bias. First the Hubbard interaction is switched off for the test of the calculation precision for a chain of $L_S=40$ without the special bond. The corresponding lengths ($L-L_S$) of ideal leads attached to the chain has been tested to be long enough so that the results are sufficiently insensitive to it. The incoming and outgoing currents are defined as the corresponding currents at the left and right interfaces according to Eq. (2), respectively. At $U=0$, the spin and charge currents are the same since no interaction between electrons of different spins exists. A time lag between the incoming and outgoing currents is observed due to the spin or charge transportation from the left chain end to the right one. After some scattering between lead and Hubbard chain due to the finite sizes, which shows a weak oscillation, the steady transport is finally reached at $t=40(\hbar/t_0)$.

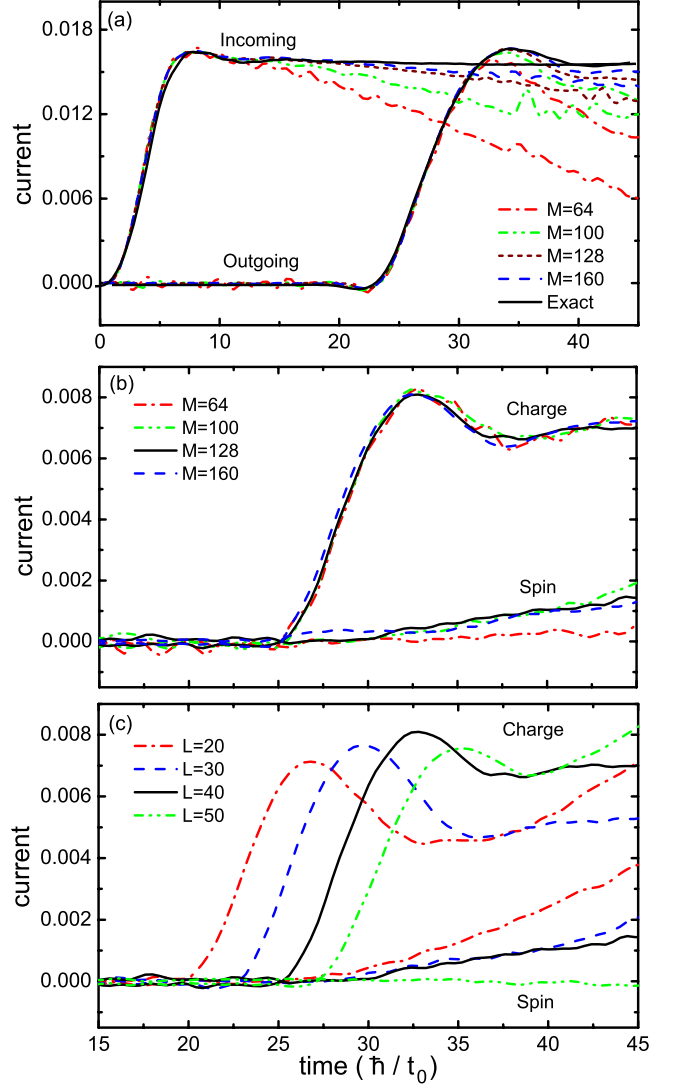


FIG. 4. (Color online) The spin and charge currents at various times for different numbers of kept DMRG states (M) or Hubbard chain lengths (L_S). (a) Both incoming and outgoing spin or charge currents are shown for $U=0$ and $L_S=40$. (b) Only the outgoing currents are shown for $U=8t_0$ and $L_S=40$. (c) The outgoing currents for different chain lengths L_S , and $U=8t_0$ and $M=160$.

In Fig. 4(a), we also show the results obtained from the t-DMRG method by keeping various numbers of DMRG states. It can be seen that the curves obtained when the number of kept DMRG states (M) is 128 or more are very close to the exact one (solid lines), while the convergence for the outgoing current is faster than that of the incoming one, the reason being that the voltage bias is applied only at the left interface for convenience in this calculation.

Next, in Fig. 4(b) we show both spin and charge outgoing currents for a Hubbard chain with the special bond for a number of different kept DMRG states (M). It is clearly seen that the convergence for a Hubbard chain is much better than that of the $U=0$ chain with increasing the number of kept DMRG states (M). In a sufficiently long time, it can be seen that while the charge current passes through the chain the spin current is blocked and only a little of it passes. This

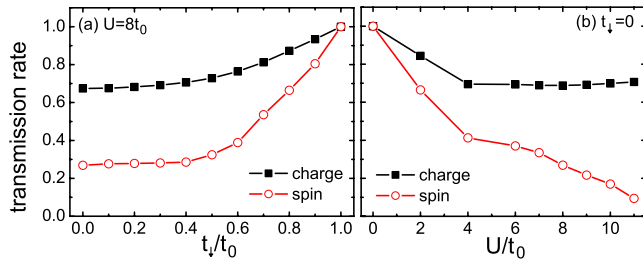


FIG. 5. (Color online) The dependence of transmission rates (see text for definition) on (a) t_{\perp} ($U=8t_0$) and (b) U ($t_{\perp}=0$).

result is consistent with the spread of a wave packet studied above. In Fig. 4(c) we give the currents for different lengths (L_S). We observe that a Hubbard chain of moderate length $L_S(=30-40)$ is optimal, for a shorter chain is accompanied by a serious finite-size effect and a longer chain by a large accumulated error since it takes more time for spin or charge to travel from one end to the other.

Finally, we give the dependence of spin or charge transport through the Hubbard chain on t_{\perp} and U in Fig. 5. The transmission rates are defined as the ratio between transmitted and incident currents, where the former is taken from the average value of the outgoing current at a period when the current is almost steady and the latter is the same of the incoming current at the period before the current reaches the right end. Figure 5(a) shows that the transmission rate changes little for $t_{\perp} < 0.5$, while Fig. 5(b) that the Hubbard

repulsion U plays a crucial role in the observed spin-current blockade. When U increases, the charge transmission rate changes little for $U > 4t_0$, and the spin rate decreases very quickly and reaches about 0.1 for $U > 10t_0$, where the spin current is nearly completely blocked by the special bond.

In the end before summary, we mention the proposal by Kollath *et al.*²⁰ to observe experimentally the spin-charge separation in cold Fermi gases, in which the temperature should be low enough ($k_B T$ being much smaller than the Mott energy gap) to ensure that thermal activation does not destroy the Mott-insulating behavior. But this is not required in our case since the Mott gap is zero. Furthermore, an important advantage is that the spin-current blockade could be realized by adjusting only one parameter (t_{\perp}), which simplifies experimental observation.

In summary, we have investigated the spin and charge transport in a Hubbard chain with a bond of controllable electronic hopping. We find the spin current can be controlled by this special bond while charge current passes through the bond freely. It is found that a large Hubbard U is required for the observed blockade since the spin-charge separation plays a crucial role in it.

This work was supported by the NSF of China, the MST of China (Grant No. 2006CB921302), the Western Institute of Nanoelectronics, and the EC Project OFSPIN (Grant No. NMP3-CT-2006-033370).

*cqwf@fudan.edu.cn

¹T. Giamarchi, *Quantum Physics in One Dimension* (Oxford University, New York, 2004).

²P. W. Anderson, *The Theory of Superconductivity in the High-Tc Cuprates* (Princeton University, Princeton, NJ, 1997).

³C. L. Kane and M. P. A. Fisher, Phys. Rev. Lett. **68**, 1220 (1992); Phys. Rev. B **46**, 15233 (1992).

⁴M. N. Baibich, J. M. Broto, A. Fert, F. Nguyen Van Dau, F. Petroff, P. Etienne, G. Creuzet, A. Friederich, and J. Chazelas, Phys. Rev. Lett. **61**, 2472 (1988).

⁵For a review, see G. A. Prinz, Phys. Today **48** (4), 58 (1995).

⁶C. Kim, A. Y. Matsuura, Z.-X. Shen, N. Motoyama, H. Eisaki, S. Uchida, T. Tohyama, and S. Maekawa, Phys. Rev. Lett. **77**, 4054 (1996); T. Lorenz, M. Hofmann, M. Grüninger, A. Freimuth, G. S. Uhrig, M. Dumm, and M. Dressel, Nature (London) **418**, 614 (2002); O. M. Auslaender, H. Steinberg, A. Yacoby, Y. Tserkovnyak, B. I. Halperin, K. W. Baldwin, L. N. Pfeiffer, and K. W. West, Science **308**, 88 (2005); B. J. Kim, H. Koh, E. Rotenberg, S.-J. Oh, H. Eisaki, N. Motoyama, S. Uchida, T. Tohyama, S. Maekawa, Z.-X. Shen, and C. Kim, Nat. Phys. **2**, 397 (2006).

⁷For a review, see I. Bloch, Nat. Phys. **1**, 23 (2005).

⁸Gavin K. Brennen, Carlton M. Caves, Poul S. Jessen, and Ivan H. Deutsch, Phys. Rev. Lett. **82**, 1060 (1999); Olaf Mandel, Markus Greiner, Artur Widera, Tim Rom, Theodor W. Hänsch, and Immanuel Bloch, *ibid.* **91**, 010407 (2003).

⁹A. Recati, P. O. Fedichev, W. Zwerger, and P. Zoller, Phys. Rev. Lett. **90**, 020401 (2003).

¹⁰S. R. White and A. E. Feiguin, Phys. Rev. Lett. **93**, 076401 (2004).

¹¹A. J. Daley, C. Kollath, U. Schollwöck, and G. Vidal, J. Stat. Mech. Theor. Exp. (2004), P04005.

¹²S. R. White, Phys. Rev. Lett. **69**, 2863 (1992); Phys. Rev. B **48**, 10345 (1993).

¹³M. Suzuki, Prog. Theor. Phys. **56**, 1454 (1976).

¹⁴D. Gobert, C. Kollath, U. Schollwöck, and G. Schütz, Phys. Rev. E **71**, 036102 (2005).

¹⁵C. Kollath, U. Schollwöck, J. von Delft, and W. Zwerger, Phys. Rev. A **71**, 053606 (2005).

¹⁶A. J. Daley, S. R. Clark, D. Jaksch, and P. Zoller, Phys. Rev. A **72**, 043618 (2005).

¹⁷R. A. Molina, D. Weinmann, R. A. Jalabert, G. L. Ingold, and J. L. Pichard, Phys. Rev. B **67**, 235306 (2003).

¹⁸V. Meden and U. Schollwöck, Phys. Rev. B **67**, 035106 (2003).

¹⁹S. Andergassen, T. Enss, C. Karrasch, and V. Meden, arXiv:cond-mat/0612229 (unpublished).

²⁰C. Kollath, U. Schollwöck, and W. Zwerger, Phys. Rev. Lett. **95**, 176401 (2005).

²¹ t_{\perp} should be a decrease function of the intersite distance, which is $\sqrt{a^2+4b^2} \sin(\theta/2)$, where a is the lattice constant and b is the interchain distance (see Ref. 8).

²²D. Weinmann, W. Häusler, and B. Kramer, Phys. Rev. Lett. **74**, 984 (1995).

²³A. Auerbach, *Interacting Electrons and Quantum Magnetism* (Springer, New York, 1998).